Paper No. 22

THE RESPONSE OF A QUARTZ CRYSTAL MICROBALANCE TO A LIQUID DEPOSIT

A. P. M. Glassford, *Lockheed Palo Alto Research Laboratories, Palo Alto, California*

ABSTRACT

Theory has been developed for predicting the loss of response of a QCM to a liquid deposit due to viscous effects in the deposit. The loss of response is expressed by a response factor, equal to the response of the QCM to a liquid film divided by its response to a solid film of the same mass per unit area. The theory assumes a droplet-type deposit morphology, and considers the influence of droplet distribution parameters. Experiments have been conducted to examine the validity of the theory, using DC 704 silicone oil as the subject deposit material. Experiments were made in two series - one with constant deposit mass and variable temperature, the other with variable deposit mass and constant temperature. Satisfactory agreement with the theory was found. Interpretation of the data using the theory has enabled information on droplet area coverage and number density to be deduced.

INTRODUCTION

The quartz crystal microbalance (QCM) has been used in the aerospace industry for several years to monitor the build-up of condensed contaminant deposits on spacecraft surfaces in both simulation and flight situations. Also, the QCM is being used increasingly in basic research on contamination-related phenomena and its accuracy and behavior in this application have consequently been subject to critical analysis. One of the areas of concern is the response of the QCM to liquid deposits, as opposed to solid deposits. Because the dynamic coupling of a liquid deposit to the crystal surface is less than one hundred per cent, the sensitivity of the QCM, measured in frequency change per unit added mass per unit area, is reduced. This is a significant problem in the aerospace contamination measurement application because many of the species outgassed from common materials, e.g. RTV silicone adhesives and potting compounds, as well as common diffusion pump oils exist as very low vapor pressure liquids at near ambient temperatures. It is therefore desirable to develop a technique for predicting the response of the QCM to liquid deposits quantitatively.

When a liquid deposit is oscillated in shear by the QCM measuring crystal only the liquid layer in immediate contact

with the crystal moves with the same velocity as the crystal surface. Liquid layers some distance from the surface can move only in response to a shear stress in the liquid, which requires a velocity gradient to be established. The presence of a velocity gradient means that the average deposit velocity during oscillation will always be less than that of the crystal surface. It has been shown elsewhere[1][2] that the frequency change of the QCM produced by an added mass is a function of its kinetic energy. Since a solid deposit moves throughout with the same velocity as the crystal surface, the change in frequency produced by an added liquid mass will always be less than that produced by an added solid mass of the same magnitude.

A further reduction in QCM response is produced by the tendency of liquid deposits to occur as a distribution of droplets. The formation of a droplet from an equivalent mass uniformly distributed over the same base area will increase the mean distance from the deposit mass to the crystal surface. Since the velocity of the liquid deposit decreases with distance from the crystal surface the formation of droplets will decrease the average velocity of the deposit, and hence further reduce the magnitude of the induced frequency change. The response will also be affected by the droplet size and number per unit area. For a given deposited mass per unit area the response of a system of a large number of small size droplets will be greater than that of a few large size droplets, because of the greater average distance of the deposit from crystal surface in the latter case. Also, the measured mass per unit area will vary with the number of droplets per unit area for a given droplet size.

The approach taken in this paper to estimate the magnitude of these effects is to determine the velocity profile of the oscillating liquid deposit, and then to derive the QCM response using the Rayleigh energy method for harmonically oscillating systems. The problem is addressed theoretically in three stages. First, the effect of viscosity is determined for a uniform liquid deposit. Second, the effect of droplet geometry is derived. Third, the effect of droplet size and distribution is investigated. A limited experimental program was then conducted to assess the validity of the derived theory.

QCM Response

The sensitivity of a QCM, S, is defined as the relationship between the added solid mass per unit area, $(\Delta m/A)_s$, and the resulting change in frequency, Δf_s. Hence for a solid mass

$$\Delta f_s = S_s \times (\Delta m/A)_s \qquad (1)$$

This paper is not concerned with the absolute sensitivity of the QCM to liquid deposits, but with the relative loss of sensitivity if the deposit is liquid rather than solid. This can

be expressed by a "response factor", F, defined as the frequency change, induced by a liquid deposit Δf_ℓ, divided by the frequency changed induced by a solid deposit of the same mass per unit area. Hence, for liquid films the relationship equivalent to (1) is

$$\Delta f_\ell = S_\ell x \, (\Delta m/A)_\ell \tag{2}$$

and, for $(\Delta m/A)_s = (\Delta m/A)_\ell$

$$F = S_\ell / S_s = \Delta f_\ell / \Delta f_s \tag{3}$$

F can be derived using the same Rayleigh energy method for undamped harmonically oscillating systems as was used successfully[1] [2] to derive the absolute sensitivity, S. In this method the total kinetic energy, T, and potential energy, V, of the system are expressed in terms of the displacements, u_i, in each degree of freedom, as follows

$$T = \tfrac{1}{2}a\left(\dot{u}_1^2 + \dot{u}_2^2 \ldots\ldots \dot{u}_n^2\right) \tag{4}$$

$$V = \tfrac{1}{2}c\left(u_1^2 + u_2^2 \ldots\ldots u_n^2\right) \tag{5}$$

The frequency of the system, f, is then given by

$$f^2 = c/a \tag{6}$$

For small perturbations of the system, such as the addition of mass to the QCM crystal, equation (6) can be rewritten

$$(f + \Delta f)^2 = (c + \Delta c)/(a + \Delta a) \tag{7}$$

The surface of a crystal oscillating in thickness shear is an antinode, so mass added there does not affect the potential energy of the system, making Δc zero. Ignoring squares of small quantities, equation (7) can be rewritten as

$$\Delta f/f = -\Delta a/a \tag{8}$$

Equation (8) can be written for solid and liquid deposits. Noting that f and a are independent of the phase of the deposit, the following expression is obtained for F from (3) and (8).

$$F = \Delta a_\ell / \Delta a_s \tag{9}$$

The response factor is thus determined from the ratio of kinetic energy coefficients of the liquid and solid deposits. These coefficients are determined from an equation similar to (4). The oscillating crystal and deposit is a single degree of freedom system, so the velocity of the system can be represented by the velocity at a single location. The logical location to select in this context is the crystal surface. In general,

oscillation velocity and deposit density can vary across the crystal and these variations can be represented by a distribution function.[2] The effect of non-uniform distribution functions is to introduce a multiplicative constant into the expression for T and hence a. Since the present analysis is concerned with comparing equivalent situations this constant would appear in both denominator and numerator of the right-hand side of equation (9), making F independent of the distribution functions. In this paper the distribution functions are thus assumed equal to unity to minimize algebraic complexity of intermediate expressions in the following derivations. A general expression for the kinetic energy of a deposit, ΔT, can then be written in terms of a uniform crystal surface velocity, $v_o \sin 2\pi ft$

$$\Delta T = \tfrac{1}{2}\Delta a (v_o \sin 2\pi ft)^2 \qquad (10)$$

The problem is now to obtain expressions for the kinetic energies of the liquid and solid deposits. This is done by integrating the kinetic energy throughout the deposit, for which the velocity distribution in the deposit must be known. The solid has the same velocity throughout, equal to that of the oscillating crystal surface. The velocity in the liquid deposit will vary through the thickness and must be determined by viscous theory.

VELOCITY DISTRIBUTION IN THE DEPOSIT

Uniform Film Deposit

Figure 1a shows the model for the oscillatory motion of a uniform liquid film. The fluid motion in the film is described by the Navier-Stokes equations. For the present case there are no pressure gradients or body forces, and flow takes place only in the y-direction. The Navier-Stokes equations thus reduce to:

$$\frac{\partial v}{\partial t} = \frac{\mu}{\rho} \cdot \frac{\partial^2 v}{\partial x^2} \qquad (11)$$

This equation is to be solved for the boundary conditions:

$$x = 0,\ v = v_o \sin 2\pi ft \quad \text{(crystal surface velocity)}$$

$$x = x_m,\ \frac{\partial v}{\partial x} = 0 \quad \text{(zero shear stress at outer boundary)}$$

Equation (11) and the above boundary conditions are whol analagous to the heat conduction problem of a parallel sided

infinite slab with harmonically varying temperature at one surface with the other surface insulated. Carslaw and Jaeger give the following solution to this problem[3], translated here into momentum transfer terms.

$$B = \left| \frac{\cosh k(x_m - x)\,(1+i)}{\cosh kx_m(1+i)} \right| \tag{12}$$

$$\phi = \arg\left(\frac{\cosh k(x_m - x)\,(1+i)}{\cosh kx_m(1+i)} \right) \tag{13}$$

$$k = \left(\frac{2\pi f \rho}{2\mu} \right)^{\frac{1}{2}} \tag{14}$$

$$v/v_o = B \sin(2\pi ft + \phi) \tag{15}$$

B is the amplitude of the oscillation at a distance x from the crystal surface while ϕ is the phase angle by which the displacement at this location trails that at the crystal surface. Numerical values of B and ϕ are given in Figure 2 as functions of kx_m and x/x_m. Equation (12) can be expanded as follows:

$$v/v_o = B\cos\phi \sin 2\pi ft + B\sin\phi\cos 2\pi ft \tag{16}$$

The velocity of the liquid thus consists of a component $B\cos\phi \sin(2\pi ft)$ in phase with the crystal motion which contributes to the inertial energy of the system, and a component $B\sin\phi\cos(2\pi ft)$ 90 degrees behind the crystal motion which contributes to the damping of the crystal motion. Although damping is not included in the Rayleigh theory, its effect will be negligible for small deposit thicknesses, since $\sin\phi \sim 0$. At larger thicknesses, however, its effect may increase to significant proportions, as noted in the Discussion.

Droplet Deposit

Figure 1b shows the model of the motion of the oscillating liquid droplet. If surface tension forces are ignored, the motion is described by equation (11), but the boundary conditions are now:

$$v = v_o \sin 2\pi ft \text{ at } x = 0,$$

and

$$\frac{\partial v_t}{\partial n} = 0 \text{ at all points on the droplet surface}$$

where v_t is the tangential velocity on the droplet surface, and n is the coordinate normal to the surface. The solution to

equation (11) with the above boundary conditions will be much more complex than for the uniform film, because the variable droplet geometry requires the introduction of more descriptive parameters. A solution to this problem has not been located in the literature, and hence for the present purposes the velocity distribution in a droplet of height x_m will be assumed to be the same as that in a uniform film of thickness x_m. In fact, the actual velocity at a given distance from the crystal surface should be higher in the droplet than in the uniform film, because the effect of area reduction with distance in the droplet will be to reduce the velocity gradient needed to exchange momentum with the outer levels of the droplet. The loss of QCM response calculated using the uniform film velocity profile will therefore be greater than the actual loss.

DETERMINATION OF THE RESPONSE FACTOR

It was noted earlier that the loss of sensitivity of the QCM to a liquid deposit is due to three effects which act together but which are conceptually separable: viscous effects, droplet formation, and droplet distribution. In the interest of clarity of presentation, these three effects are considered one at a time in the following analysis. F is derived in turn for the uniform liquid film, individual liquid droplets and then distributed liquid droplets.

In the theoretical analysis, F is shown to be primarily a function of the distance of the deposit from the QCM surface, while the primary data output from the QCM is mass per unit area. To connect the theory with experimental data, the concept of nominal deposit thickness, ℓ_n, is used. ℓ_n is defined as the deposit mass per unit area divided by the density. Further, it was shown in the viscous flow analysis above that distance from the QCM surface to points in the deposit can be non-dimensionalized by multiplying them by k, equation (14). The theoretical expressions for F are thus developed as functions of $k\ell_n$. The following paragraphs present the derivation of the kinetic energy of the various deposits, ΔT. Finally, in order to simplify the algebra, ΔT is derived per unit area, permitting the crystal area to be eliminated from the integrations.

Uniform Film Deposit

For the uniform solid deposit the velocity throughout is equal to that of the crystal surface. The kinetic energy per unit crystal surface area, ΔT_{su} is given by

$$\Delta T_{su} = \tfrac{1}{2}\rho \int_o^{x_m} (v_o \sin 2\pi ft)^2 \, dx \qquad (17)$$

$$= \tfrac{1}{2}\rho \; x_m \; (v_o \sin 2\pi ft)^2$$

By comparison with equation (10), the kinetic energy coefficient per unit area, Δa_{su}, is given by

$$\Delta a_{su} = \rho x_m \tag{18}$$

The kinetic energy of the uniform liquid deposit, $\Delta T_{\ell u}$ will be a function of the component of the local velocity in phase with the inertia forces, $v_o B \cos\phi \sin 2\pi ft$.

$$\begin{aligned} \Delta T_{\ell u} &= \tfrac{1}{2}\rho \int_o^{x_m} (v_o \cos\phi \sin 2\pi ft)^2 \, dx \\ &= \tfrac{1}{2}\rho \int_o^{x_m} (B \cos\phi)^2 \cdot dx \, (v_o \sin 2\pi ft)^2 \end{aligned} \tag{19}$$

By comparison with equation (10)

$$\Delta a_{\ell u} = \rho \int_o^{x_m} (B \cos \phi)^2 \, dx \tag{20}$$

From equations (9), (18) and (20) the response factor for a uniform film, F_u, is thus

$$\begin{aligned} F_u &= \int_o^{x_m} (B \cos \phi)^2 \, dx / x_m \\ &= \int_o^1 (B \cos \phi)^2 \, d(x/x_m) \end{aligned} \tag{21}$$

F_u has been computed from equations (12), (13) and (21) for various values of kx_m, and is plotted in Figure 3 as a function of $k\ell_{nu}$, noting that for a uniform film ℓ_{nu} is equal to x_m. The shape of the curve represents a transition from the very small response loss for small deposits ($k\ell_{nu} < 0.2$) to the asymptotic response of a quasi-infinite film ($k\ell_{nu} > 1.6$) which is almost totally confined to the region near the crystal and is thus independent of nominal thickness. Also plotted in Figure 3 is the product $F_u \cdot k\ell_{nu}$, which is proportional to the actual QCM output. The rising of this QCM output function to a maximum, followed by a steady decline is the most commonly encountered practical manifestation of QCM viscous effects.

Single Droplets

Whereas the geometry of a uniform film can be characterized by a single dimension, several geometric parameters are necessary for the specification of condensed droplets. Since

the purpose of this paper is to demonstrate the credibility of the analysis rather than perform an analysis of droplet geometry some simplifying assumptions are made. The droplet is assumed to have the form of a spherical cap with contact angle θ_c and height x_m. Relationships between area, volume and x_m and θ_c are derived in the Appendix.

For a solid droplet of volume V_d and base area A_d the kinetic energy per unit base area, ΔT_{sd}, is given by

$$\Delta T_{sd} = \tfrac{1}{2}\rho \int_o^{x_m} A(x)\,(v_o \sin 2\pi ft)^2\,dx/A_d$$

$$= \tfrac{1}{2}\rho\,(V_d/A_d)\,(v_o \sin 2\pi ft)^2 \qquad (22)$$

Hence, from (A6), (A9) and (10),

$$\Delta a_{sd} = \rho \frac{x_m}{3}\left(\frac{2 - \cos\theta_c\,(2+\sin^2\theta_c)}{(1-\cos\theta_c)\sin^2\theta_c}\right) \qquad (23)$$

For a liquid droplet of the same dimensions, the kinetic energy per unit base area, $\Delta T_{\ell d}$, is (assuming that the velocity profile is given by equation (15))

$$\Delta T_{\ell d} = \tfrac{1}{2}\rho\int_o^{x_m} A(x)\cdot(v_o B\cos\phi \sin 2\pi ft)^2 dx/A_d$$

$$= \tfrac{1}{2}\rho\int_o^{x_m} A(x)/A_d)\,(B\cos\phi)^2\,dx\cdot(v_o \sin 2\pi ft)^2 \qquad (24)$$

From equations (10), and (24)

$$\Delta a_{\ell d} = \rho\int_o^{x_m} (A(x)/A_d)\,(B\cos\phi)^2\,dx \qquad (25)$$

Hence from equations (9), (23) and (25)

$$F_d = \frac{3\sin^2\theta_c\,(1-\cos\theta_c)}{(2-\cos\theta_c(2+\sin^2\theta_c))}\int_o^1 (A(x)/A_d)(B\cos\theta)^2 d(x/x_m) \qquad (26)$$

In order to evaluate F_d for the purposes of illustration of the effect of droplet and/or comparison with the experimental data of the next section, it is necessary to know the value of θ_c. θ_c depends on several parameters, such as temperature and

surface condition, and data relevant to the present situation are not available. However, photomicrographs made by the author of similar deposits showed contact angles near 30°, and it can be shown by evaluating equations (A5) and (A6) that the function $A(x)/A_d$ varies little for $10° < \theta_c < 50°$. So that the derived equations may be evaluated a value of θ_c equal to 30° has thus been assumed. F_d has been computed from equation (26) for various values of kx_m using θ_c equal to 30°, and equations (12), (13), (A5) and (A6). The nominal deposit thickness of the droplet, ℓ_{nd} relative to its own base area, A_d is given by

$$\ell_{nd} = V_d/A_d = 0.512\, x_m \qquad (27)$$

where V_d and A_d are given by equations (A12) and (A11). F_d is plotted versus $k\ell_{nd}$ in Figure 4. While the relationship is qualitatively similar to that for the uniform film, the effect of configuring a liquid deposit as a droplet is shown to be a further decrease in the response of the QCM for a given nominal thickness.

Distribution of Droplets

A real liquid deposit will consist of a distribution of droplets of various sizes and spacings. The effect of droplet spacing will be to cause the deposit mass per unit area of QCM crystal - the quantity sensed by the QCM - to be lower than the mass per unit droplet base area. Assuming all droplets to be the same size, the nominal deposit thickness for the distributed droplets, ℓ_{ndd}, is related to the nominal thickness of the droplet referred to its base area, ℓ_{nd}, by an area coverage factor, α_A:

$$\ell_{ndd} = \alpha_A \times \ell_{nd} \qquad (28)$$

where

$$\alpha_A = \frac{\text{area covered by droplets}}{\text{total QCM area}} = A_d N_d \qquad (29)$$

The response factor, F_{dd}, is a function only of droplet geometry, not the distribution, and thus is given by equation (26) as a function of kx_m. However, the computed value of F_{dd} is now plotted versus $k\ell_{ndd}$, given as follows (from equations (27) and (28)).

$$k\ell_{ndd} = \alpha_A \times 0.512\, kx_m \qquad (30)$$

Figure 4 shows a family of curves of F_{dd} versus $k\ell_{ndd}$ for various values of α_A. In practice α_A has a maximum value of

$\pi/4$ cos 30 or 0.907, corresponding to a close packed hexagonal distribution. Another significant value of α_A is 0.785, for a close packed square distribution. The QCM response is seen to fall with decreasing area coverage.

PRACTICAL APPLICATION OF THE THEORY

The single fundamental output from a QCM with an added mass is change of frequency. A solid, evenly distributed deposit can be characterized by a single parameter-mass per unit area - and the QCM sensitivity is constant. Hence, a single frequency change data point can be translated into an added mass. However, unless the deposit mass is small enough for F to be near to unity, a liquid deposit requires several parameters to be determined, such as droplet shape and size and area distribution, and liquid viscosity. Hence several data points are required for determination of the deposit parameters, which precludes direct unequivocal measurement of the mass of a particular liquid deposit. The most appropriate use of the theory appears to be in the analysis of processes made up of a series of data points from which the various parameters can be deduced. Two situations of this type occur quite frequently in practice. In one situation a QCM with a deposit on its surface is warmed up with no loss or rearrangement of deposit. In this situation k varies, while the geometric parameters ℓ_{ndd}, A_d, V_d, and α_A remain constant. Thus the response factor F_{dd} varies with $k\ell_{ndd}$ at constant α_A, and the QCM response during warm-up should follow one of the constant α_A characteristics of Figure 4. In the other situation the QCM is held at constant temperature while the accumulation or loss of deposit is measured, in which case k is constant, while the geometric parameters vary. It is suggested that during condensation a liquid droplet deposit builds up by growth of the individual droplets at constant distribution density, N_d, until adjacent droplets touch and coalesce, thereby reducing N_d and increasing the spacing between droplets. Growth resumes at constant N_d until coalescing occurs again. In practice, the droplets will have a distribution of sizes and spacings, so a succession of discrete steps in N_d are unlikely. A more likely process is growth at constant N_d from an initial condition of relatively widely and randomly spaced nucleation centers, until the droplets begin to coalesce, whereafter N_d adjusts continuously downwards while the deposit maintains a more or less close packed arrangement. Characteristic paths can be derived for this postulated process as follows. Equations (28) and (29) can be combined to give

$$k\ell_{ndd} = A_d \cdot N_d \cdot k\ell_{nd} \tag{31}$$

For θ_c equal to 30°, noting (27), (31) and (A6)

$$k\ell_{ndd} = 167\,(N_d/k^2)\cdot(k\ell_{nd})^3 \qquad (32)$$

The relationship between F_{dd} and $k\ell_{ndd}$ for isothermal growth at constant N_d/k^2 is found by determining F_{dd} for a given $k\ell_{nd}$ from equations (26) and (27), and $k\ell_{ndd}$ from equation (32) for constant values of N_d/k^2. These constant N_d/k^2 characteristics are shown in Figure 4. According to the suggested mechanism growth will occur along one or more lines of constant N_d/k^2 until a close packed situation occurs, at which point N_d will decrease and growth will continue along another line, constant N_d/k^2.

EXPERIMENTAL INVESTIGATIONS

The validity and usefulness of the theory presented above was examined by a series of experiments using Dow Corning DC 704 silicone oil on a Celesco Model 700 quartz crystal microbalance. Noting the remarks in the previous section, two types of experiments were conducted. In the first type the response of constant temperature QCM to a steadily increasing deposit was measured. In the second type a deposit was formed on the QCM and then its response was measured as a function of temperature.

Apparatus

The apparatus is shown schematically in Figure 5. The QCM can be maintained at any desired temperature above 77°K by balancing the electric power into a resistance heater wound. on the holder against heat lost through a thermal link between holder and shroud. Also mounted within the shroud but shielded from the QCM by a cooled partition is a pot containing DC 704. The pot temperature can be maintained at any temperature above 77°K by balancing electrical heater power against a thermal l. The pot has an orifice whose axis lies along the line between pot and QCM permitting a flux of DC 704 molecules to be directed at the QCM sensing crystal through a hole in the partition, which can be closed by a remotely controlled shutter. The whole apparatus is mounted in a glass bell jar, evacuatable to pressures below about 2×10^{-7} torr.

Viscosity of DC 704

In order to determine k for an experimental situation, the relationship between the viscosity of the subject liquid must be known as a function of temperature. Figure 6 shows kinematic viscosity versus temperature obtained from the Dow Corning Company.[4] DC 704 is a phenyl-methyl siloxane, a high molecular weight silicone oil related to the general family of polydimethyl siloxanes, which have been shown to exhibit non-Newtonian flow behavior at high shear rates.[5] The shear

rates experienced by a liquid deposit on a oscillating QCM can be quite high, and could conceivably reach the order of magnitude required for non-Newtonian behavior to occur. The possibility of this situation being reached in the present experiments is covered in the Discussion.

QCM Response Data

In the first series of tests the QCM was held at constant temperature while its surface was exposed to a constant flux of DC 704 molecules. The test was begun with the QCM surface clean. The shutter was then opened and the QCM output recorded as a function of time. Data interpretation was based on the assumption that after the initial adsorption and nucleation processes were completed, the condensation rate could be assumed to be constant. This constant actual condensation rate was determined from the initial indicated condensation rate, since the response factor for small nominal thicknesses is essentially unity. The actual mass per unit area on the QCM at later times in the deposition was then calculated from the assumed constant condensation rate and the time since the beginning of exposure. The accuracy of this linear extrapolation was confirmed by interrupting the flux and cooling the QCM at the conclusion of the test in order to regain full response of the deposit by solidification. The agreement between this final measurement and the magnitude predicted by the linear extrapolation was surprisingly good -- always better than five percent, and usually no worse than one percent. The response factor was calculated as a function of deposit thickness by dividing the indicated mass per unit area by the calculated mass per unit area for the same instant of time. The nominal thickness was found from the calculated mass per unit area and the density, while k was found for the test temperature from equation (14) and Figure 6. Data from four experiments of this type, performed for QCM temperatures of 27°C, 37°C, and 51°C, are plotted in Figures 7 and 8. The experiment at 37°C was repeated for two net condensation rates -- 0.61×10^{-8} and 1.22×10^{-8} gms/cm^2/sec. The data for 27°C and 51°C were obtained for net condensation rates of 1.53×10^{-8} and 1.72×10^{-8} gms/cm^2/sec, respectively. The data for 27°C and 37°C appear to follow the scenario proposed in the previous section. For the early stages of growth ($k\ell_n < 0.25$) the data appear to follow roughly two N_d/k^2 characteristics, with a transition near $k\ell_n \sim 0.1$. For $0.25 < k\ell_n < 0.5$ the process occurs along a more or less close-packed characteristic. The departure of the data from the theoretical close packed characteristics for $k\ell_n > 0.5$ is probably due to the increasing significance of effects neglected in the present analysis, and is covered in the Discussion. The number of droplets per unit area in these deposits can be estimated by fitting theoretical constant N_d/k^2 curves to the data for $0.05 < k\ell_n < 0.25$, using equation (31) or Figure 4.

At 37°C, for which k is 11687 cm^{-1}, the data can be fitted by N_d/k^2 equal to about 0.045, making N_d of the order of $6x10^6$ cm^{-2}. At 27°C, for which k is 9474 cm^{-1}, N_d/k^2 equal to 0.04 is a reasonable fit, making N_d about $4x10^6$ cm^{-2}. Use of these values for N_d at 51°C, where k is equal to 14980 cm^{-1} indicates that corresponding values of N_d/k^2 at 51°C should be in the range of about 0.03 to 0.02. Constant N_d/k^2 curves for these values have been drawn on Figure 8, showing that 51°C data do fall in this range, even though the shape of the data is inconclusive.

These values of N_d can be compared with the photomicrographs of Shapiro and Hanyok[6], which show DC 704 deposits on various surfaces. These photomicrographs show number densities in the range of $5x10^5$ to $1x10^6$ cm^{-2} for deposits on a mirror surface, which, because of its smoothness would be expected to have somewhat fewer nucleation sites than the QCM surface.

In the second series of tests deposits of different magnitudes were condensed on the QCM and their response measured as a function of temperature. The true mass per unit area of each deposit was found by cooling the QCM below the solidification temperature, which was near -35°C. The response at other temperatures was determined by heating or cooling the QCM through a series of equilibrium temperatures. This technique is limited to temperatures below the region in which re-evaporation rate of the DC 704 became significant, which was about 20°C. The response factor at a given temperature was calculated from the mass per unit area indicated by the QCM at that temperature divided by the true mass per unit area. The nominal thickness was found from the actual mass per unit area divided by the density. k was variable in these tests and was calculated from equation (14) and Figure 6. The data for several experiments with different nominal thicknesses are shown in Figure 9. The maximum value of $k\ell_n$ reached in each test was determined by either the attainment of a temperature at which the re-evaporation rate became significant (about 20°C) or an abrupt loss of output occurred, the possible cause of which is suggested in the Discussion. It was noted in the previous section that the deposit geometry should remain constant during these tests, in which case the data should follow the constant α_A characteristics of Figure 4. The data do indeed follow the same general pattern as the theoretical curves, although they appear to show a slightly faster decline at high values of $k\ell_n$. However, the data for the $5.12x10^{-5}$ cm deposit shows the same inflection point near $k\ell_n$ of 0.4 as predicted by theory, this being the only set of data in which the inflection point was observed.

The slightly different shape of the data curves from the constant α_A curves of Figure 4 is thought to be due to temperature dependent effects ignored in the theory, for example, droplet shape or constant angle. It was first thought that the

discrepancy might have depended on the temperature at which the deposit was formed. A deposit formed on a cold QCM may have a continuous film morphology, which breaks down into droplets as heating occurs. To investigate this possibility several experiments were made with a 6.54×10^{-5} cm film thickness. In one experiment the deposit was formed cold (-45°C) and the data were acquired during heating. In a second experiment an equivalent deposit was formed near 20°C and data were obtained during cooling, then by reheating and recooling. The data from these two series of tests shown in Figure 9 are virtually indistinguishable.

It was concluded from these data that a transition from continuous film to droplet geometry, or any other irreversible geometric change does not occur in the temperature range studied, even if the deposit is formed in the solid phase. This means that the surface mobility of DC 704 at -45°C is sufficient to produce a morphology similar to that obtained for liquid phase deposition.

The deposit nominal thicknesses used in these tests was quite high, so that sufficiently large values of $k\ell_n$ could be reached. It is possible that the thicknesses were high enough to cause the deposit morphology to begin to differ from the distributed, even sized droplet pattern assumed with apparent success for smaller nominal deposit thicknesses. This possibility was assessed using the following relationship, which can be derived from equations (27), (29), (30), and (A6).

$$\alpha_a = 5.5 \cdot \ell_{ndd}^{2/3} \cdot N_d^{1/3} \qquad (33)$$

The data for ℓ_{ndd} equal to 1.75×10^{-5} cm can be fitted quite well by the theoretical curve for α_A equal to 0.6, Figure 4. Insertion of these numbers in equation (33) gives N_d equal to 4.2×10^6 -2 cm which is in good agreement with the earlier data, and tends to confirm the validity of the model for this nominal thickness. The data for 5.12×10^{-5} cm for $k\ell_{ndd} < 0.25$ can be fitted by α_A equal to about 0.8, while for $k\ell_{ndd} > 0.25$ a better fit is obtained for α_A equal to 0.70. These α_A values correspond to N_d values of 1.2×10^6 -2 cm and 8.0×10^5 -2 cm, respectively, and also suggest that at this thickness the deposit is approaching a close packed situation. The data for the 6.54×10^{-5} cm deposit at $k\ell_{ndd} < 0.3$ can only be fitted by α_A equal to unity, which is impossible for a droplet deposit, for which α_A cannot exceed 0.91. This seems to indicate that a transition to a more film-like morphology is occurring at these higher nominal thicknesses, which is to be expected.

DISCUSSION

The intent of this paper was to demonstrate that the variable response of the QCM to liqui deposits can be explained almost totally by viscous effects coupled with a droplet type deposit morphology. It is apparent from the agreement obtained between the theory and the experiments that this has been satisfactorily achieved. Good qualitative and quantitative agreement was obtained up to non-dimensional nominal thicknesses of about 0.5. Above this value a very rapid fall off in response was experienced in all tests where this $k\ell_n$ value was reached. Detail analysis of the experimental data in this region revealed a discontinuity in the second differential of F versus $k\ell_n$, indicating a change of controlling phenomenon. It is suggested that this could be due to the onset of non-Newtonian effects in the silicone oil, or a change in the modal response of the oscillating crystal under the higher damping forces which will arise with heavier deposits. The oscillation amplitude of the crystal is of the order of 50Å,[7] so that for a deposit of nominal thickness of 1000 Å on a 10MHz crystal the shear rate is of the order of $(10^7 x 2 x 50)/1000$ or 10^6 sec^{-1}. This is well within the range in which silicone fluids can show a sharp loss of apparent viscosity. However, a detailed analysis of the velocity profile in the deposit, plus viscosity data for DC 704 at high shear rates would be needed to investigate this point further. Assessment of the possibility of modal changes is beyond the scope of this work.

Although the quantitative agreement between the theory and the data appears to be quite good, it should be re-emphasized that several major assumptions were made. These were:

(1) Use of the uniform film velocity profile for the liquid droplet.
(2) Assumption of spherical-cap droplet shape and uniform droplet size distribution.
(3) Neglection of damping effects in the Rayleigh frequency perturbation analysis.
(4) Exclusion of all other possible surface forces except viscous drag from the analysis.
(5) To permit reduction of the data the viscosity data obtained from Dow Corning were arbitrarily extrapolated from about -12°C to about -35°C.

It is logical to suppose that refinements of the analysis in these areas would produce better agreement with the experiment.

It was noted in the text that it is not possible to use the theory to interpret isolated data points because of the many parameters involved. Instead the utility of the theory will probably be to generate insight into condensation and revaporation processes. Interpretation of the data presented in this paper has generated credible values for area coverage and

number density for the droplet and has suggested that the spherical cap shape assumption may be acceptable. Further work in which some of the neglected effects are included in the analysis, coupled with more careful, systematic experimental measurements may well prove to be a fruitful source of data on contamination deposit morphology.

NOMENCLATURE

A_d	Droplet base area
a, Δa	Rayleigh kinetic energy coefficient
B	Oscillation velocity magnitude
c, Δc	Rayleigh potential energy coefficients
F	QCM response factor
f	QCM frequency
k	$(2\pi f\rho/2\mu)^{\frac{1}{2}}$
ℓ_n	Deposit nominal thickness
$(\Delta m/A)$	Deposit mass per unit area
N_d	Number of droplets per unit area
r	Solid radius of spherical cap droplet
S	QCM sensitivity
T	Rayleigh total kinetic energy
u	Rayleigh displacement coordinate
V	Rayleigh total potential energy
V_d	Droplet volume
v	Local velocity in deposit
v_o	Maximum crystal surface velocity
x	Distance between QCM surface and a point in the deposit
x_m	Distance between QCM surface and the most distant point in the deposit
α_A	Fraction of QCM surface covered by droplets
ϕ	Phase angle of motion in the deposit
θ_c	Droplet contact angle
μ/ρ	Kinematic viscosity of the deposit
ρ	Deposit density

Subscripts:

l	droplet
dd	distributed droplet
ℓ	liquid
n	nominal
s	solid
u	uniform

REFERENCES

1. Stockbridge, C.D., "Resonant Frequency Versus Mass Added to Quartz Crystals," Vacuum Microbalance Techniques, Vol. 5, 1966, Plenum Press, N.Y., K. Behrndt, pp. 193-206.

2. Glassford, A.P.M., "Analysis of the Accuracy of a Quartz Crystal Microbalance," Paper No. 76-438, AIAA 11th Thermophysics Conference, San Diego, California, July 1976.

3. Carslaw, H.S., and Jaeger, J.C., "Conduction of Heat in Solids," Oxford University Press, 2nd Edition, 1959, Chapter III, Section 3.6.

4. Private Communication from A.J. DeSapio, Dow Corning Company, Sept. 1975.

5. Lee, C. L., Polmanteer, K. E., and King, E.G., "Flow Behavior of Narrow Distribution Polydimethyl Siloxane," Journal of Polymer Science; Part A2, Vol. 3 (1970) pp. 1909-1916.

6. Shapiro, H., and Hanyok, J., "Monomolecular Contamination of Optical Surfaces," Vacuum, Vol. 18, No. 11, (1968), pp. 587-592.

7. Stockbridge, C.D., "Effect of Gas Pressure on Quartz Crystal Microbalances," Vacuum Microbalance Techniques, Vol. 5, 1966, K. Behrndt ed., pp. 147-178.

APPENDIX

The principal geometric parameters of the spherical cap droplet are indicated in Figure 10. Other parameters may be derived as follows:

Droplet height, x:

$$x = r(\cos\theta - \cos\theta_c) \tag{A1}$$

$$x_m = r(1 - \cos\theta_c) \tag{A2}$$

Hence
$$x = x_m(\cos\theta - \cos\theta_c)/(1 - \cos\theta_c) \tag{A3}$$

Droplet cross-sectional area, A(x):

$$A(x) = \pi(r\sin\theta)^2 \tag{A4}$$

Obtaining r^2 from A2 and $\sin^2\theta$ from A3

$$A(x) = \frac{\pi x_m^2}{(1 - \cos\theta_c)^2}\left[1 - \left((x/x_m)(1-\cos\theta_c) + \cos\theta_c\right)^2\right] \tag{A5}$$

Base area, A_d (= A(x) at $x/x_m = 0$):

$$A_d = \frac{\pi x_m^2 \sin^2\theta_c}{(1 - \cos\theta_c)^2} \tag{A6}$$

Volume, V_d:

$$V_d = \int_o^{x_m} A(x) \cdot dx \tag{A7}$$

Substituting A4 in A7

$$V_d = \frac{\pi r^3}{3} \left[2 - \cos\theta_c (2 + \sin^2\theta_c) \right] \tag{A8}$$

Substituting A2 in A8

$$V_d = \frac{\pi x_m^3}{3} \left[\frac{2 - \cos\theta_c (2 + \sin^2\theta_c)}{(1 - \cos\theta_c)^3} \right] \tag{A9}$$

For θ_c equal to 30^o the following relationships follow from A5, A6 and A9.

$$A(x) = 175\, x_m^2 \left[1 - (0.134(x/x_m) + 0.886)^2 \right] \tag{A10}$$

$$A_d = 43.8 x_m^2 \tag{A11}$$

$$V_d = 22.4\, x_m^3 \tag{A12}$$

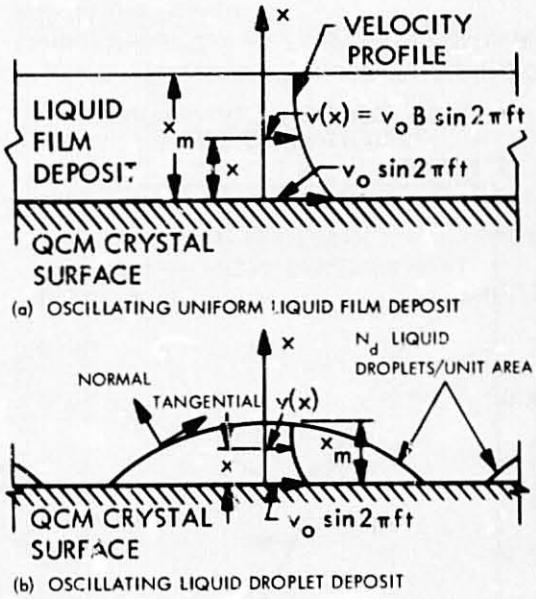

Figure 1. Schematic of Uniform and Droplet Liquid Deposits.

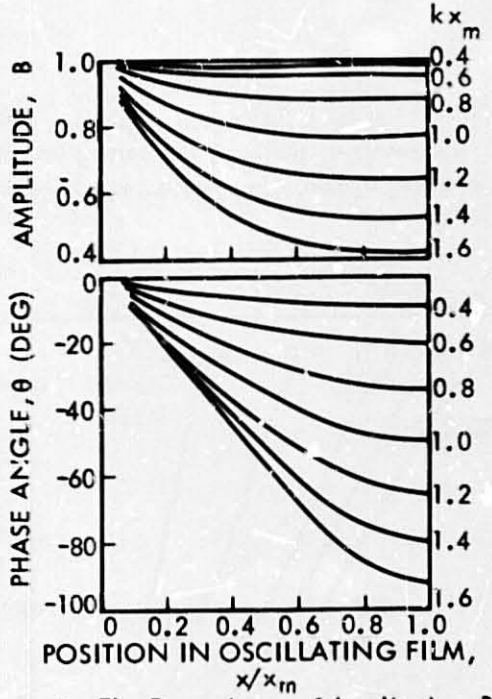

Figure 2. The Dependence of Amplitude, B, and Phase Angle θ, on Position in the Liquid Film, x/x_m and Non-Dimensional Thickness, kx_m, for an Oscillating Liquid Film.

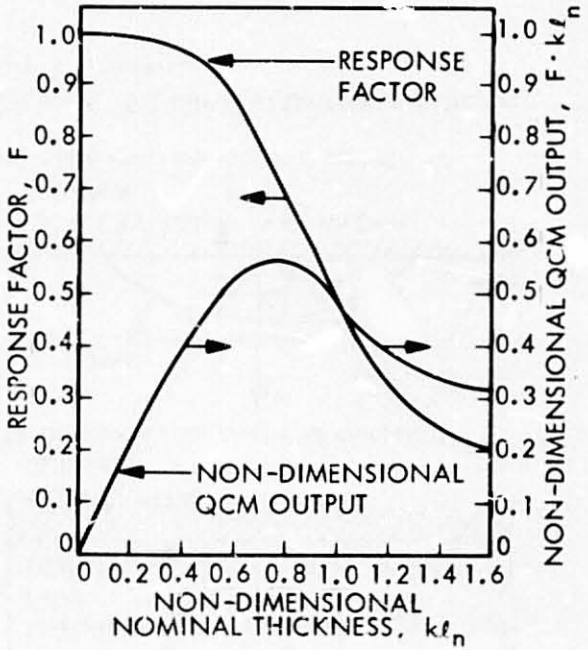

Figure 3. Theoretical Response Factor and QCM Output Versus Deposit Thickness for Uniform Film Liquid Deposit.

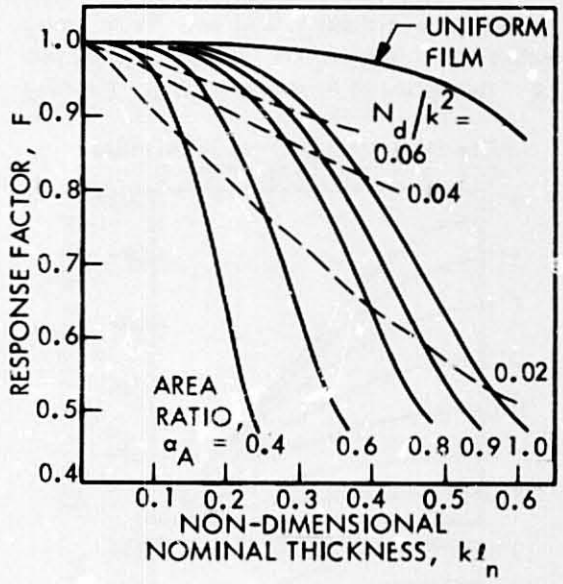

Figure 4. Theoretical Relationship Between Response Factor and Nominal Thickness for Liquid Droplet Deposits ($\theta_c = 30^o$).

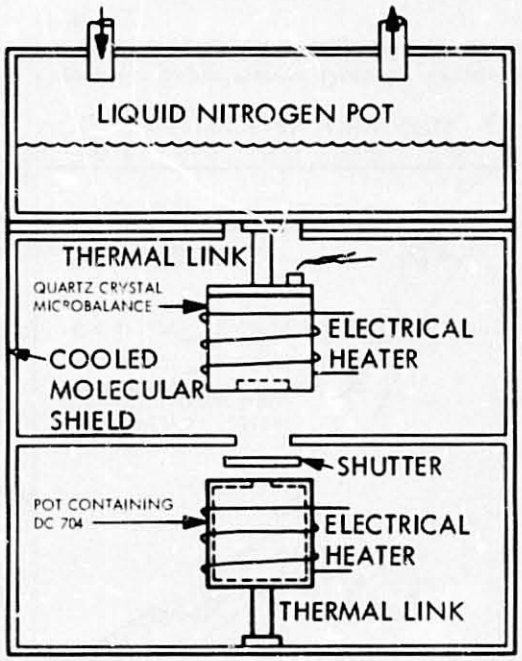

Figure 5. Experimental Apparatus.

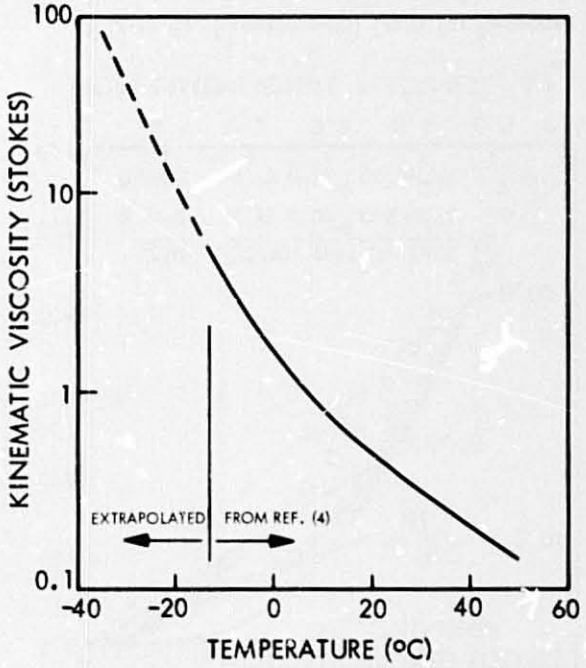

Figure 6. Viscosity of DC 704 Silicone Oil

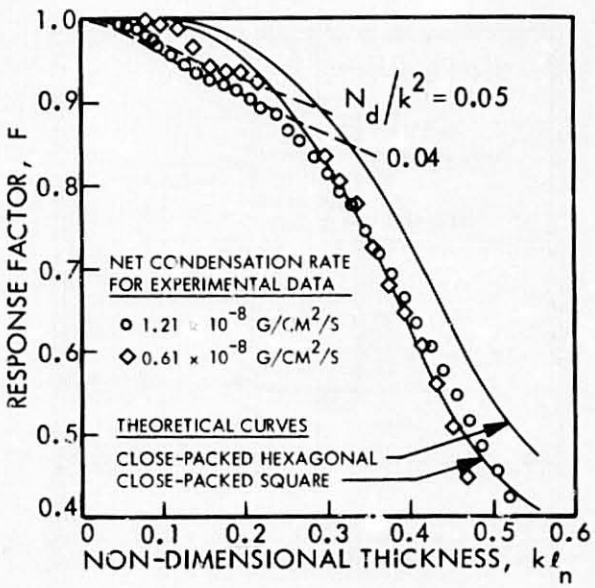

Figure 7. Experimental Data for Response Factor as a Function of Deposit Magnitude at 37°C.

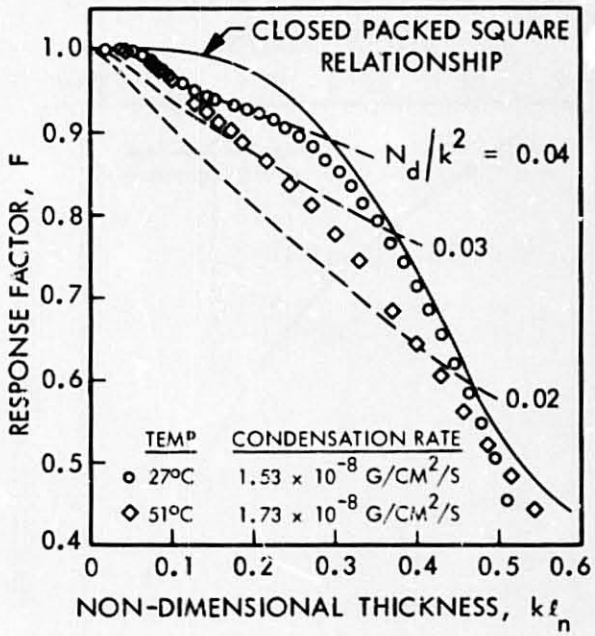

Figure 8. Experimental Data for Response Factor as a Function of Deposit Magnitude at 27°C and 51°C.

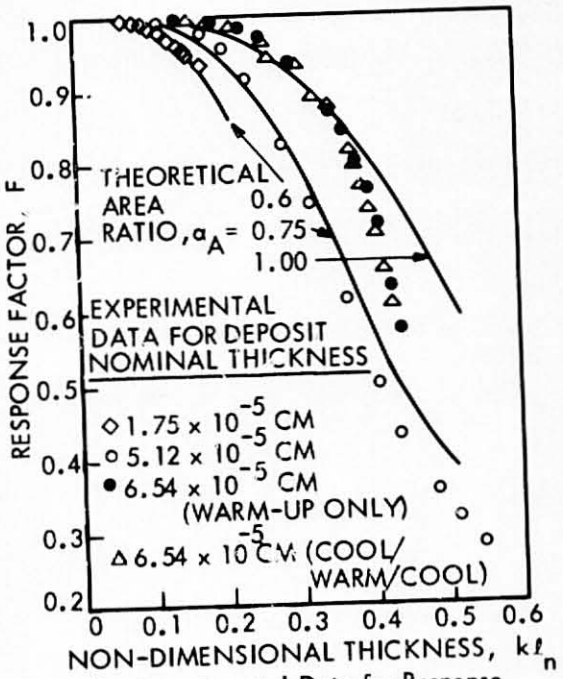

Figure 9. Experimental Data for Response Factor as a Function of $k\ell_n$ for Three Values of Nominal Thickness.

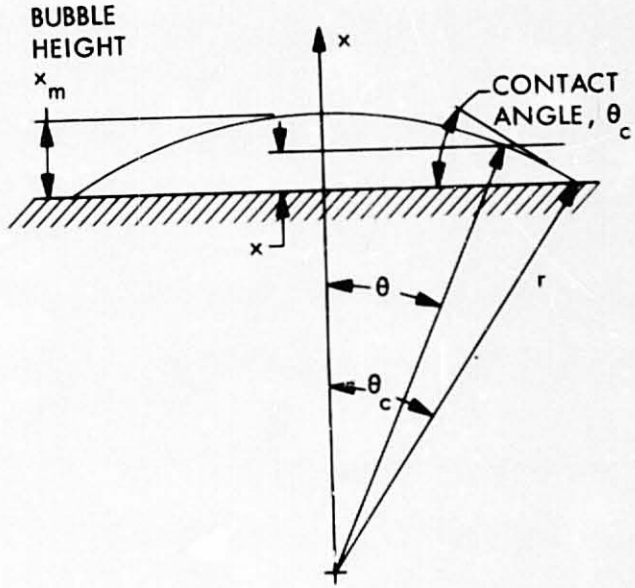

Figure 10. Major Dimensions of a Spherical Cap Droplet on a Surface.